Artificial Linear Brush Abrasion of Coatings for Photovoltaic Module First Surfaces

Jimmy M. Newkirk, [1] Illya Nayshevsky, [2,3] Archana Sinha, [4] Adam Law, [5] QianFeng Xu, [6] Bobby To,[1] Paul F. Ndione, [1] Laura T. Schelhas, [4] John M. Walls, [5] Alan M. Lyons, [2,3,6] David C. Miller [1*]

[1]National Renewable Energy Laboratory, Golden, CO, USA
[2]College of Staten Island, City University of New York, Staten Island, NY, USA
[3]The Graduate Center, City University of New York, New York, NY, USA
[4]SLAC National Accelerator Laboratory, Menlo Park, CA, USA
[5]Loughborough University, Loughborough, United Kingdom
[6]ARL Designs LLC, New York, NY, USA
[*]Presenter (David.Miller@nrel.gov)

International PV Soiling Workshop (https://www.PVSoiling-Workshop.org)
Wednesday, 2019/10/30, 11:00-11:25
Ras El Hanout conference room, Radisson Blu hotel, Marrakech, MA

NREL/PR-5K00-75028

Motivation

- PV now uses AR and/or AS coatings to increase electricity generation and reduce effects of soiling.
- ~1%·day^{-1} performance loss in MENA ⇒ clean PV modules daily.

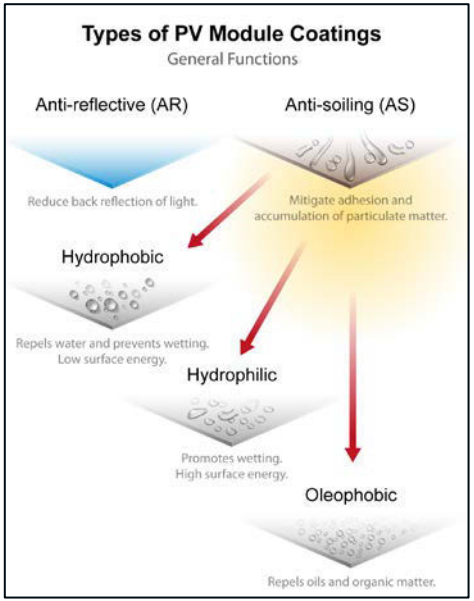

Coatings used on PV front surfaces.
Einhorn et. al., J PV, 9, 2018, 233-239.

Vendor cleaning building glazings (at NREL campus).

- Much of the damage to coatings results from cleaning.
- PV leverages cleaning methods and equipment from the building glazing industry.

For linear artificial brush method in IEC 62788-7-3 PV abrasion standard:

⇒Compare durability of popular coating types.

⇒Compare rate- and damage characteristics between wet & dry dust abrasion.

⇒Compare rate- and damage characteristics for other factors affecting abrasion.

Summary of Standardized Artificial Machine Abrasion Test Methods

- Most recent Taber tester (BS EN 1096-2) applies greater contact pressure than brush tests (which most closely resemble equipment & methods used to clean PV).

TEST METHOD	INDUSTRY OF ORIGIN	ABRASIVE MATERIAL	SIZE ABRASIVE (GEOMETRY) {mm}	NOMINAL CONTACT PRESSURE {kPa}	STROKE LENGTH {mm}	*n*, NUMBER OF CYCLES {dimensionless}	CYCLE REPEAT SPEED {cpm}
BS EN 1096-2 (Annex E) [9]	bulding glazings	felt or grit embedded rubber tip	14.5 or 7 (diameter)	24.2 or 103.9	120	500	60
ASTM D2486 [10]	paints	wet Nylon 6 bristles plus silica, surfactant slurry	35 x 85 (area); 19 (length) & 0.30 (Æ)	1.5	270	pre-condition brush 400 cycles; test 400 cycle increments to failure	37
DIN 53778-2 [11]	paints	wet hogs bristle plus sodium-n-dodecylbenzenesulphonate in water	38 x 89 (area); 10.5 (length)	0.7	270	pre-condition brush 1000 cycles; test # cycles to failure	not specified
ISO 11998 [12]	paints	wet steel wool pad plus sodium-n-dodecylbenzenesulphonate in water	39 x 90 (area); 38 (thick)	not specified	300	pre-soak; 200 cycles	37
ASTM D4213 [13]	paints	wet steel wool pad plus cellulose, surfactant slurry	77 x 97 (area); 6 (thick)	not specified	255	pre-soak; 200 cycle increment test up to 800 cycles	not specified
ASTM D3450 [14]	architectural coatings	damp cellulose sponge with silica, surfactant slurry	76 x 95 (area); 38 (thick)	2.0	not specified	0, 25, 50, 75, 100	37
ASTM D4828 [15]	paints	unspecified sponge	not specified	not specified	255	100	37
UN/ECE Regulation 43 [16]	automotive glazings	chloroprene rubber wiper blade plus ISO 12103 A4 dust	11 (length)	not specified	130	10k plus 10k cycles	37
ISO 15082 [17] ISO 20566 [18] UN/ECE Regulation 43 [16]	automotive glazings	polyethylene brush plus 24 mm ∅ silica slurry	440 (long) & 0.8 (Æ) bristles	not specified	>300	10 cycles	30 cpm (linear) 127 rpm (rotation)
ISO 3537 [19]	automotive glazings	abrasive or grit embedded wheel	12.7 (wheel width) 44.4 - 52.5 (wheel Æ)	not specified	N/A	100, 500, or 1000	rotate at 60 rpm or 72 rpm
ISO 15082 [17]	automotive glazings	Al_2O_3 or SiC grit embedded in matrix	12.7 (wheel width) 44.4 - 52.5 (wheel Æ)	not specified	N/A	100, 500, or 1000	rotate at 60 rpm or 72 rpm
ASTM D1044 [20] ASTM G195 [21]	transparent plastics general use	abrasive or grit embedded rubber wheel	12.7 (wheel width) 44.4 - 52.5 (wheel Æ)	not specified	N/A	10, 25, 50, 100; user defined	rotate at 60 rpm or 72 rpm
ASTM D4060 [22]	paints	abrasive or grit embedded rubber wheel	12.7 (wheel width) 44.4 - 52.5 (wheel Æ)	not specified	N/A	50 cycle increment test up to 500 cycles	rotate at 60 rpm or 72 rpm

building-, paints- or automotive-windows

cellulose- or silica-slurry (vs. contamination)

condition brush or scrub device (vs. extended use)

- Legacy test rate of 37 cycles per minute; 6 - 60 cpm is now commonly available.

Standardized test methods for artificial machine abrasion that *may be applied for* accelerated testing for the *cleaning of PV modules*.
Updated from Miller et. al. , NREL/TP-5J00-66334, 2016, 1-25.

Summary of Solar-Specific Artificial Machine Abrasion Studies

- BS EN 1096-2 most commonly used, despite limited present use of BAPV & BIPV ⇒ mimic building glazing industry (extended outdoor use).
- Most common abrasives: brush bristles, AZ test dust, *felt, or grit-embedded-disc products. Latter: limited fidelity to cleaning equipment.*

AUTHORS, REFERENCE	TEST METHOD	ABRASIVE MATERIAL	SIZE TEST FIXTURE (GEOMETRY) {mm}	NOMINAL CONTACT PRESSURE {kPa}	STROKE LENGTH {mm}	*n*, NUMBER OF CYCLES {dimensionless}	CYCLE REPEAT SPEED {cpm}
Bengoechea et. al. [23]	based on BS EN 1096-2	Nylon 6/6 bristles with SiO_2 sand, Aramco test dust, or silica	20 x 40 (area) 0.060ÆÆ0.200	2.5	70	200	120
Cauchois et. al. [24]	based on BS EN 1096-2	felt or grit embedded rubber tip	not specified	not specified	not specified	10, 20, 50, 100, 150, 200, 250 500, 1k, 2k, 4k, 6k, 10k	not specified
Ferretti et. al. [25] Ferretti et. al. [26]	BS EN 1096-2	grit embedded rubber	7 (diameter)	90.9	100	0, 25, 50, 250, 500, 1k	60
Ferretti et. al. [27]	custom rotary brush	CTP-300-3 Method 313 sand [28]; PA 6 bristle	0.16 or 0.42 (Æ); 40 (length) & 0.3 (Æ)	not specified	module length	1k	not specified
Klimm et. al., [29]	BS EN 1096-2	felt	14.5 (diameter)	24.2	120	0, 500, 1k, 1.5k	60
Lange et. al. [30]	ISO 11998	PA bristle; ISO 12103 A2 test dust [xxx]	35 x 85 (area) 19 mm (length);	1.5	100	0, 10 , 50, 100	72
Miller et. al. [31]	based on ASTM D2486	bristles: PA, hog bristle, PE, horsehair; ISO 12103 A4 test dust [xxx]	35 x 85 (area) 19, 38 (length) 0.30, 0.64, 0.22, 0.25 (Æ);	1.5	270	0, 100, 500, 1k, 5k, 10k, 20k	37
Pan et. al., [32]	BS EN 1096-2	felt	not specified	not specified	not specified	0, 500, 1k, 2k, 5k	not specified
Pop et. al., [33]	BS EN 1096-2	felt	14.5 (diameter)	24.2	100	0, 200, 400, 600, 800, 1k	30
Weber et. al., [34]	BS EN 1096-2	felt grit embedded rubber	7 (diameter)	103.9	100	0, 50, 100, 250, 1k	60
Womack et. al. [35] Isbilir et. al. [36] Womack et. al. [37]	BS EN 1096-2	felt grit embedded rubber	7 14.5 (diameter)	259.8 30.3 & 60.6	30	100	60

Summary of solar-specific abrasion studies in the research literature

Nominal contact pressure brush test ≤10x (less accelerated) than Taber test.

Cleaning (over 25 years)
-monthly: 300 cycles.
-weekly: 1300 cycles.
-daily: ~9k cycles.

Limitations of Existing Standards and Prior Studies

Literature studies (in general):

- Performed at ambient laboratory conditions, whereas modules can experience a wide variety of E, T, and %RH.
- Not used with weathering, artificial soiling, or cementation, but could be part of accelerated test sequence.
- Acid/base chemistry at the surface (known to affect the surface through glass corrosion) not explored in literature.

Specific to this study:

- Moderate bristle ∅ & shorter length. Accelerate relative to commercial PV brushes, i.e., ∅ of 0.25-0.50 mm & length of 3-8 cm.
- Select ISO 12103-1 AZ test dust relative to field data. A2 recommended.

Details of the Specimens Examined

- Monolithic materials (no coating): Diamant glass (typical substrate) or PMMA.
- "Materials": surface chemistry, etching, porous SiO_2, polymer, TiO_2, oxide stack
- Performance characteristics: contact angle, representative solar weighted transmittance of photon irradiance (τ_{drsw}), surface roughness

Summary of specimens examined.

SPECIMEN INDEX	COATING OR MATERIAL	COATING THICKNESS {nm}	R_a, COATING ROUGHNESS {nm}	AR	$\tau_{d,rsw}$ {%}	$\Delta\tau_{d,rsw}$ {%}	AS SURFACE FUNCTIONALIZATION	CA, CONTACT ANGLE {°}	WETTING CHARACTERISTIC
A	monolithic PMMA	no coating	3.6	no	89.2	N/A	no	70	least-hydrophilic
B	porous silica*	125	4.6	yes	91.8	1.7	yes	88	least-hydrophilic
E	porous silica*	130	25.3	yes	93.0	2.3	no	49	moderately-hydrophilic
J	monolithic glass substrate	no coating	3.4	no	90.1	N/A	no	43	moderately-hydrophilic
L	etched glass	no coating	5.5	yes	90.8	0.7	yes	50	moderately-hydrophilic
P	polymer	40	5.0	yes	90.8	0.6	yes	118	least-hydrophobic
R	silane chemistry	no coating	3.4	no	90.2	0.1	yes	102	least-hydrophobic
V	TiO_2	50	2.2	no	79.3	-7.5	yes	45	moderately-hydrophilic
Z	$ZrO_2/SiO_2/ZrO_2/SiO_2$	20/30/135/95	7.4	yes	90.2	0.1	no	9	most-hydrophilic

- I don't know of a standardized surface energy taxonomy. ☹
- Glass is inherently hydrophilic.
- Most PV industry coatings modestly affect surface energy (research grade coatings are expensive!)

Summary of surface energy classification scheme.

greatest surface energy	
$0<\theta\leq10$	most-philic
$10<\theta\leq50$	moderately-philic
$50<\theta\leq90$	least-philic
$90<\theta\leq120$	least-phobic
$120<\theta\leq150$	moderately-phobic (Wenzel state)
$150<\theta\leq180$	most-phobic (Cassie-Baxter state)
least surface energy	

Details of the Linear Artificial Brush Abrasion Tester

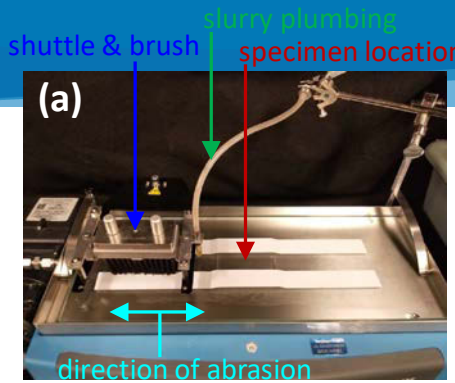

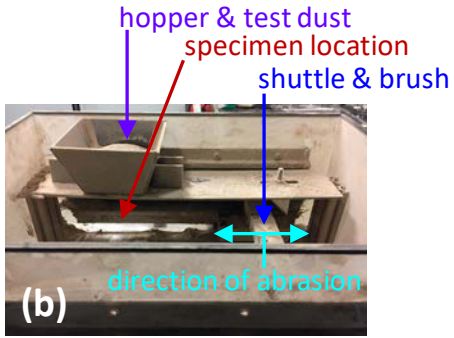

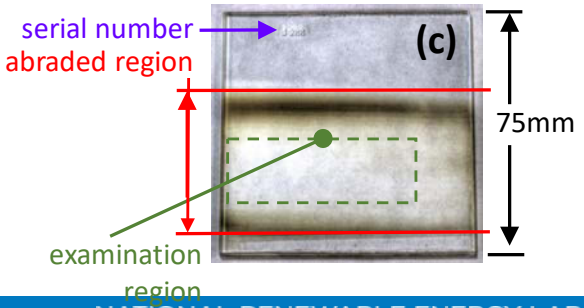

Experiments:

- Custom slurry or dry dust chambers used with commercial tester.
- Brush bristles: polyamide (Nylon 6/12), 3.8 cm length.
- A3 “medium” AZ test dust abrasive (ISO 12103-1).
- Slurry (5 $g \cdot L^{-1}$) dispensed continuously at 100 $mL \cdot min^{-1}$
- 20 mg dry dust dispensed with each cycle.

Specimen test region:

- Characterizations performed only within examination region.
- Image (c) is chosen from a previous study, providing an obvious representation of the abraded region.

Miller et. al., IEEE J PV, 2019.

-Less surface abrasion & no obvious discoloration was observed this study (longer bristles, finer abrasive, lower cycle count).

Details of the Linear Artificial Brush Abrasion Tester

- Brushes: 0.30 mm (“default”) or 0.075 mm (“soft brush”) ∅.
- Slurry dispensing rate was consistent - all coatings examined with slurry; some coatings not examined with dry dust, dry brush, and/or wet brush.
- AZ test dust not used in 2 experiments.
- All specimens were cleaned after abrasion using noncontact methods (deionized water rinse, clean dry air spray, then N_2 storage) before examination.

SPECIMEN INDEX	BRUSH	WET TEST	DRY TEST	ABRASIVE PRESENT	*n* , NUMBER OF CYCLES {dimensionless}
A	default	Y	Y	ISO 12103 A3	0, 10, 25, 50, 75, 100, 5k
B	default	Y	Y	ISO 12103 A3	0, 10, 25, 50, 75, 100, 5k
E	default	Y	Y	ISO 12103 A3	0, 10, 25, 50, 75, 100, 5k
J	default	Y	Y	ISO 12103 A3	0, 10, 25, 50, 75, 100, 5k, 10k, 20k
L	default	Y	Y	ISO 12103 A3	0, 10, 25, 50, 75, 100, 5k
P	default	Y	Y	ISO 12103 A3	0, 10, 25, 50, 75, 100, 5k
P	default	Y	Y	none	0, 10, 100, 500, 1k, 5k, 10k
P	soft bristle	Y	N	ISO 12103 A3	0, 10, 100, 500, 1k, 5k, 10k
R	default	Y	Y	ISO 12103 A3	0, 10, 25, 50, 75, 100, 5k
V	default	Y	N	ISO 12103 A3	0, 10, 100, 500, 1k, 5k, 10k, 20k
Z	default	Y	N	ISO 12103 A3	0, 10, 100, 500, 1k, 5k, 10k, 20k

Summary of the linear machine abrasion experiments performed in this study.

Characteristics Examined

- (Initial) coating thickness (ellipsometer and cross-sectional SEM)
- Visual appearance (optical microscope)
- Surface energy (contact angle, goniometer)
- Surface roughness (white light interferometer)
- Optical transmittance (spectrophotometer, no integrating sphere)
- (Select) surface morphology (AFM for scratch-width and –depth)
- (Select) chemical composition (XPS)

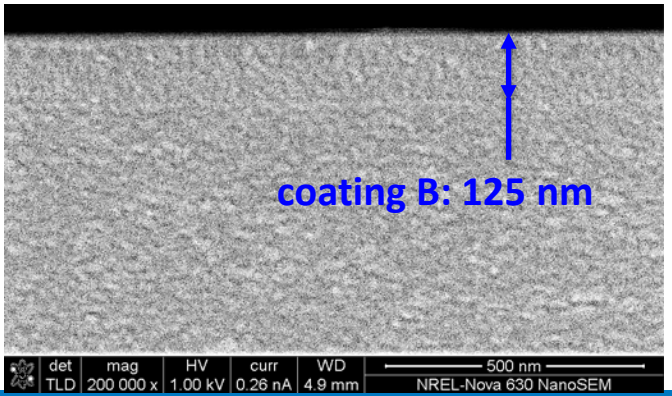

Representative electron microscopy image for coating thickness assessment (specimen B).

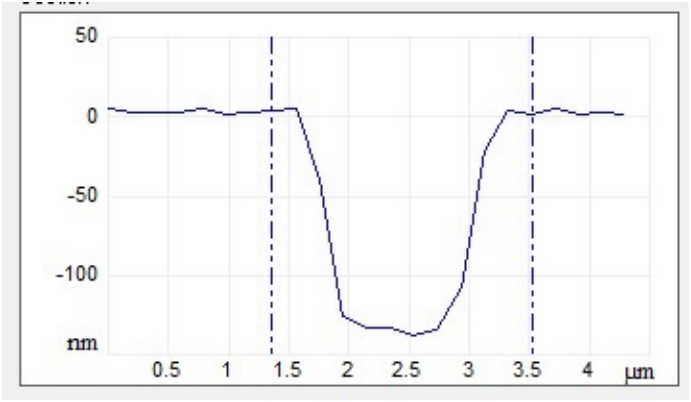

Representative profile of AFM scan for scratch size assessment (specimen B).

Representative Optical Performance of Unabraded Specimens

- Improvement in τ_d for B, E, L, P, and Z is consistent with an AR coating, applied to J (glass, with no coating).
- B, E, L, and P have a broad spectral bandwidth, consistent with a graded *n* (porous silica or etched surface). Use *n* intermediate to air and glass.
- Z optimized for CdTe PV(350 – 850 nm), not Si PV (300-2500 nm).
- *n* of TiO_2 > *n* of glass ⇒ reduced τ_d and spectral bandwidth for V.

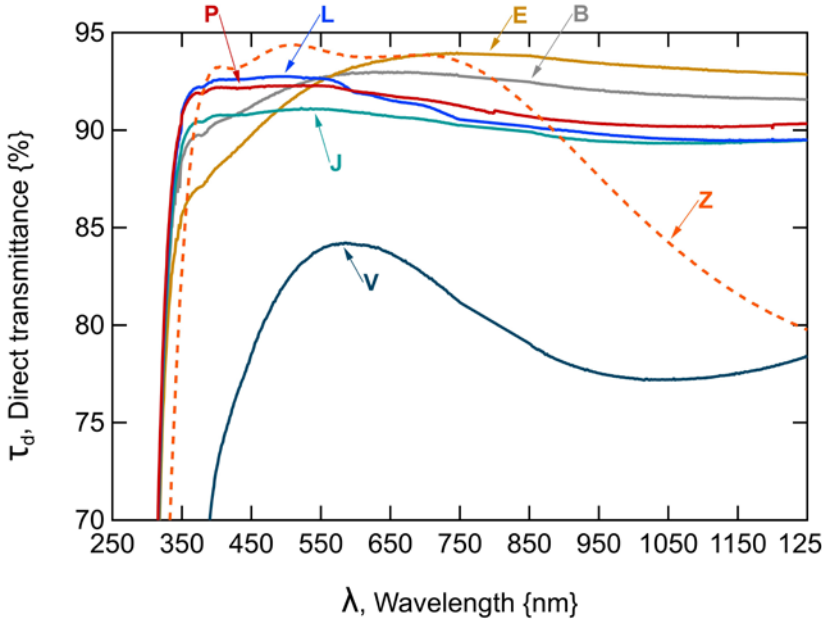

Representative direct transmittance spectra (obtained with no integrating sphere) for select untested substrate/coating specimens in this study. A subset of the transmittance (measured from 0% – 100%) and wavelengths examined (measured from 200 nm – 2500 nm) are shown.

Comparing Slurry and Dry Dust Abrasion (Transmittance and YI)

- Specimen A is most affected, including τ_d, *CA*, and R_a, making it the informal working reference material.
- Onset & magnitude of degradation greater for dry dust than slurry. Similar dust deposition rate ⇒ greater damage propensity for dry dust.

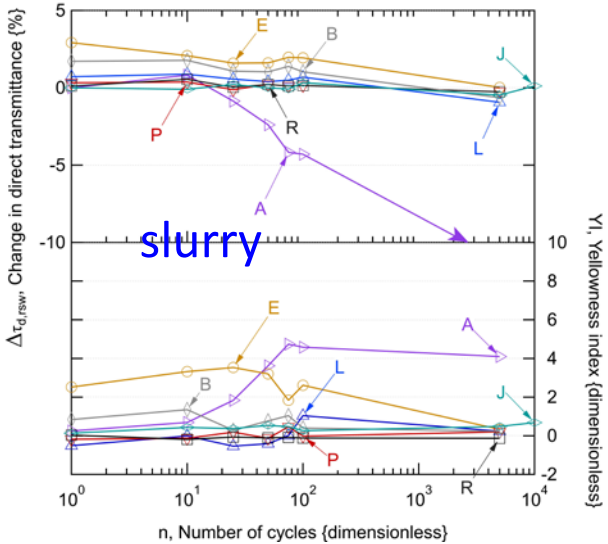

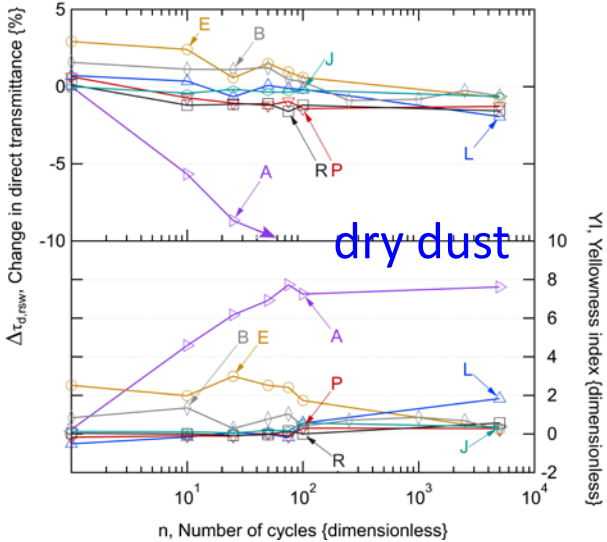

Comparison of the change in transmittance (i.e., coating optical performance) and yellowness index (which may vary with optical scattering) with the cumulative brush cycle count (n ≤ 5000) for select coatings for linear abrasion with slurry (left) and dry dust (right).

Comparing slurry and dry dust abrasion (surface energy and roughness)

- *CA* & R_a suggest longevity of the materials examined is in the order of 50 to 200 cycles for the test methods in this study.
- Loss in *CA* and/or R_a often observed before $\Delta\tau_d$ for B, E, L, and P.
- Changes in *CA* & R_a correlate for materials with a film thickness.

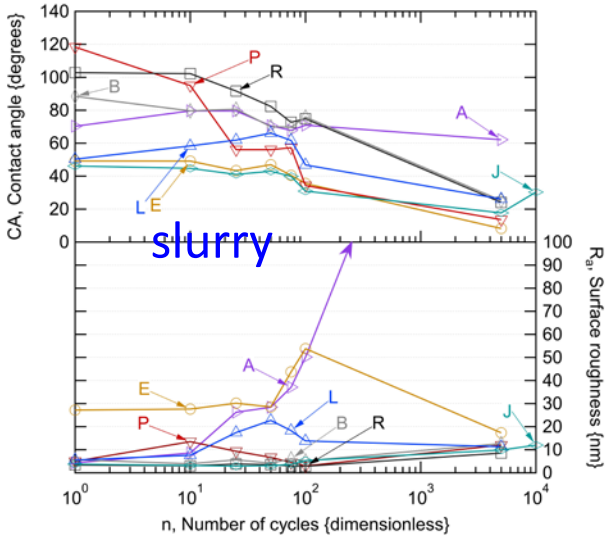

- *Greater change in* R_a and its variation for dry dust → water acts as a lubricant and facilitates heat transfer.

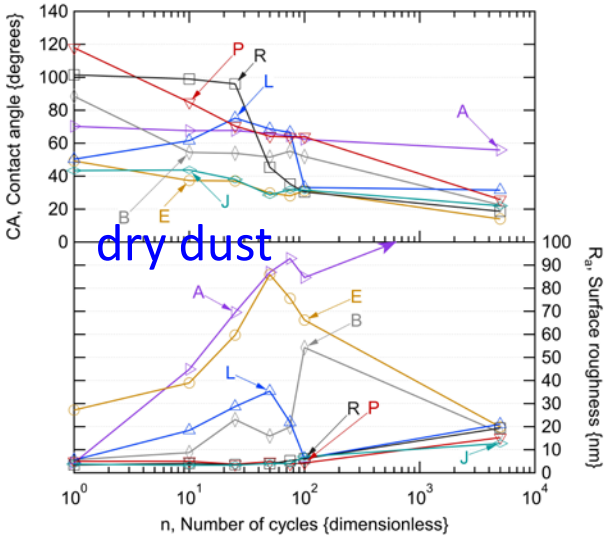

Comparison of the change in surface energy (contact angle for water) and average surface roughness with the cumulative brush cycle count (n ≤ 5000) for select coatings for linear abrasion with slurry.

Comparing effect of abrasion parameters for the same coating

- *YI*, *CA*, and R_a asymptote to J, consistent with removal of P coating.
- Coating longevity increased to 100-1000 cycles if no test dust is used.
  ⇒Majority of damage from test dust, which acts as an abrasive.
- Intermediate $P_{Soft\ Bristle}$: abrasion also affected by choice of equipment.

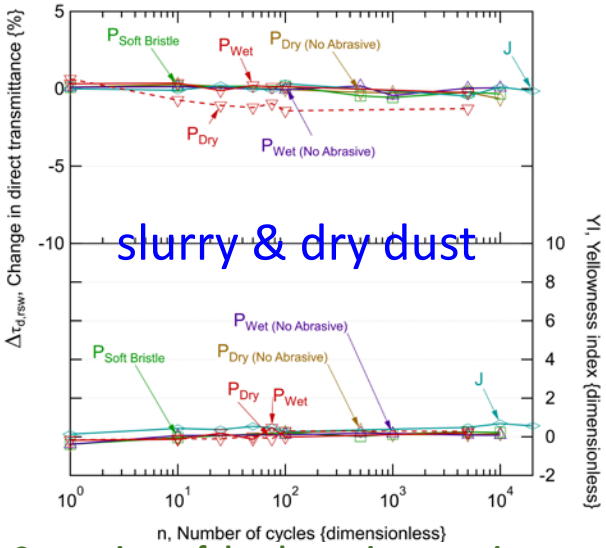

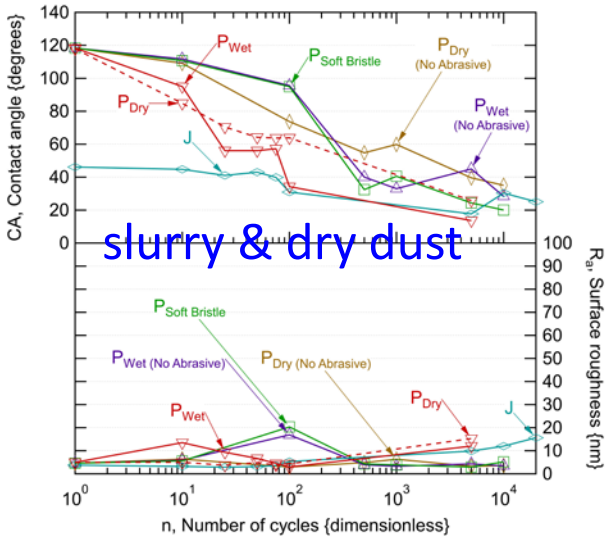

Comparison of the change in transmittance, yellowness index, surface energy, and surface roughness with the cumulative brush cycle count ($n \leq 20000$) for select coatings and test methods for linear abrasion with slurry.

Comparing the abrasion durability of different coatings

- $\tau_{d,rsw}$ increases & *YI* decreases with cycles for V (limited spectral τ of TiO_2).
- $\Delta\ \tau_{d,rsw}$, *YI*, R_a affected for Z for $n > 5k$.
- greater durability for solid dielectric coatings: V (deteriorates $500 \leq n \leq 1k$) and specimen Z ($1k \leq n \leq 5k$).

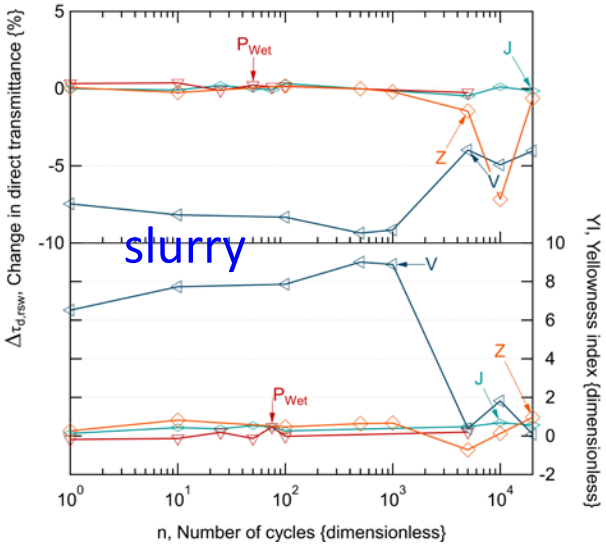

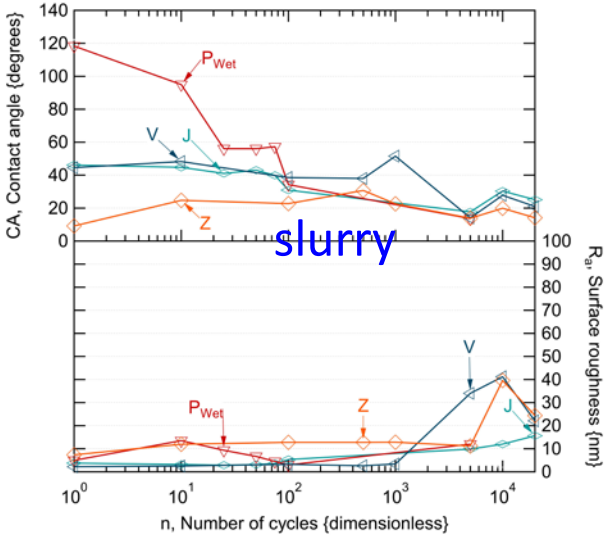

Comparison of the change in transmittance, yellowness index, surface energy, and surface roughness with the cumulative brush cycle count ($n \leq 20000$) for select coatings for linear abrasion with slurry.

Optical Microscopy Corroborates Degradation & Coating Failure

- AFM confirms bright linear features (scratches) in (b); dark features (remaining coating) in (c) and (d).

- Formation of a network of scratches followed by loss of coating is consistent with the correlation between *CA*, R_a, and τ_d, observed for specimens B, E, L, P, V, and Z.

- Distinct change in τ_d, *CA*, and R_a in some experiments suggests complete coating failure.

- Occurrence of a local maximum in R_a in some experiments may indicate fortuitous observation (appropriate # of cycles at destruction).

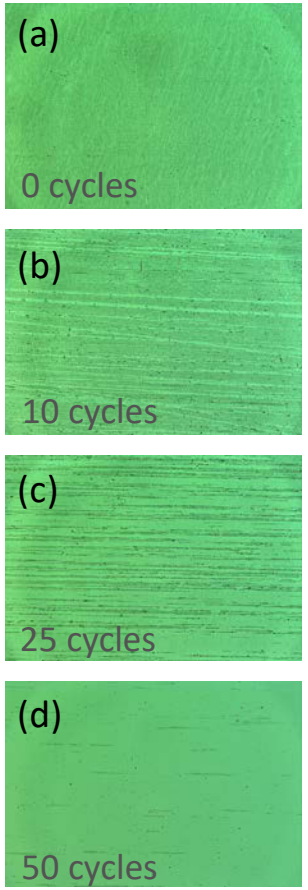

Select optical microscopy images of the P coating for linear abrasion with slurry.

AFM Identifies Similar Initial Abrasion Between Distinct Experiments

- w_s ~μm's. h_s ~tens of nm's.
- Limited width (w_s ~ min[$\varnothing_{A3\ dust}$], $w_s << \varnothing_{bristle}$) & depth ($h_s < h_n$) confirms scratches correspond to initial surface abrasion.
- w_s & h_s similar between disparate experiments (no dust, soft brush).
- ⇒Facets/edges of dust or sharp features on bristles form scratch tracks.
- Greater w_s observed for field coupons and comparable h_s observed for artificial abrasion

(see Miller et. al., J PV, in press).

COATING	TEST CONDITION	w_s, SCRATCH WIDTH (MIN-**AVG**-MAX) {μm}	h_s, SCRATCH DEPTH (MIN-**AVG**-MAX) {nm}	h_n, NOMINAL COATING THICKNESS {nm}
B	SLURRY	1.2-**2.0**-4.0	128-**136**-142	125
	DRY DUST	0.6-**1.7**-4.8	1.5-**76**-136	125
E	SLURRY	0.6-**1.8**-7.1	3.3-**42**-121	130
	DRY DUST	0.6-**1.2**-2.2	8.8-**43**-121	130
L	SLURRY	0.6-**1.0**-3.7	8.8-**34**-84	0
	DRY DUST	0.6-**2.7**-22	19-**46**-88	0
P	SLURRY	1.0-**3.3**-17	28-**38**-50	40
	DRY DUST	1.0-**4.3**-13	17-**24**-33	40
	WET BRUSH	0.6-**2.9**-8.5	12-**25**-62	40
	DRY BRUSH	0.6-**4.2**-12	20-**36**-58	40
	SOFT BRUSH (SLURRY)	0.6-**1.7**-3.7	13-**30**-55	40
J	SLURRY	0.8-**0.9**-1.2	5.1-**12**-24	0
	DRY	0.4-**0.8**-1.2	5.2-**20**-69	0

Measured scratch geometry for select specimens in the linear abrasion experiments *at 10 cycles*.

Depth-Composition Confirms the Loss of Sn, Accumulation of Al with Abrasion

- Ca, Na, and Mg (known components of float glass) observed for specimen J.
- Sn at the surface of specimens with no abrasion consistent with float glass.
- Lack of Sn suggests surface wear of at least 20 nm for abraded samples after 20k cycles.
- Al at surface of abraded specimens. Al_2O_3 present in AZ test dust.
- C suggests outer carbonaceous layer (removable by abrasion), more hydrophobic than clean glass.
- Lack of Fe at surface of the abraded specimens suggests deposition of components of AZ test dust are reduced relative to previous studies. ☺

no abrasion

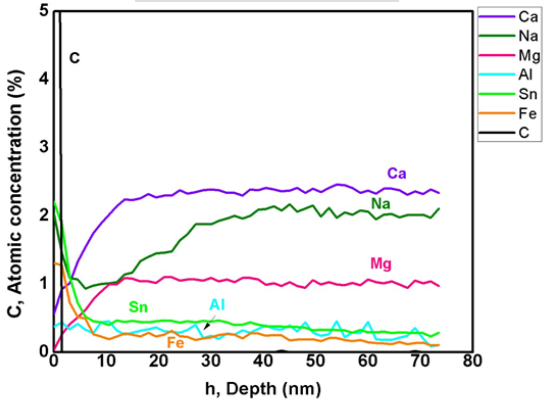

slurry test (n=20k)

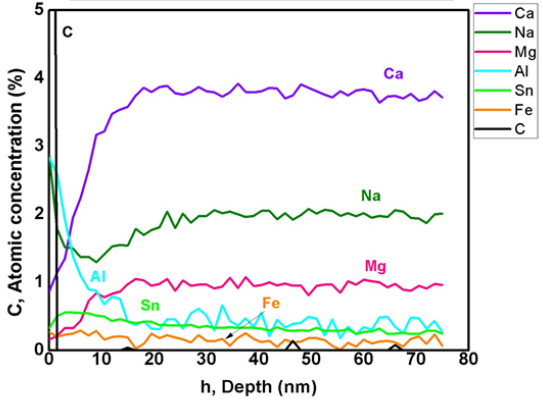

dry dust (n=20k)

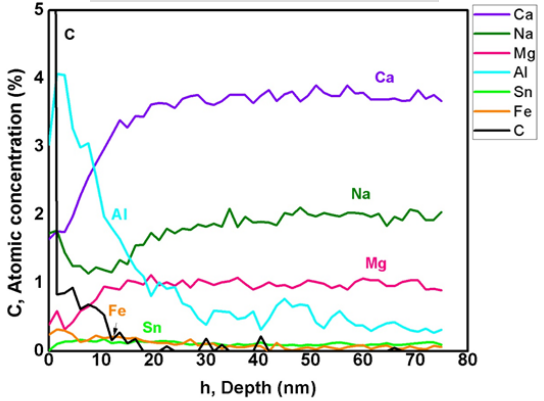

XPS depth profiling chemical composition at and near the first surface of a specimen J specimens (glass with no coating): (a) that was not abrasion tested, (b) slurry abrasion tested, and (c) abrasion tested using dry AZ test dust.

Summary & Conclusions

- Overall correlation observed between τ_d, *YI*, *CA*, and R_a consistent with: damage initiation, damage accumulation, destruction of the film, substrate abrasion (converging to characteristics of glass substrate).
- *CA* and R_a may be used for the initial detection of coating degradation (preceeding τ_d), particularly for specimens with a coating of thickness (> nm's).
- From AFM, abrasion damage primarily results from facets/edges of dust or sharp features on bristles, which provide localized damage during brush testing.
- Variety of longevities from 100 to 1000 to 10000 cycles observed.
  - -Some specimens durability consistent with use in western locations, i.e., a few cleanings per year - up to 100 cycles total.
  - -Some specimens durability consistent with use in more challenging locations (e.g., MENA), where daily cleaning may be required – in the order of 10000 cycles.
- XPS confirms details of the test parameters (A3 test dust; bristle length) improved the linear artificial brush abrasion method relative to previous study.

PVQAT TG12 (Soiling of PV)

PVQAT
International PV Quality Assurance Task Force

International PV Soiling workshop (all general topics)
- ✧ Annual in autumn.
- ✧ Contact: Lin SIMPSON <Lin.Simpson@nrel.gov>

Task Group 12 Webinars (all general topics)
- ✧ Quarterly webinars on soiling topics.
- ✧ Contact: David MILLER <David.Miller@nrel.gov>

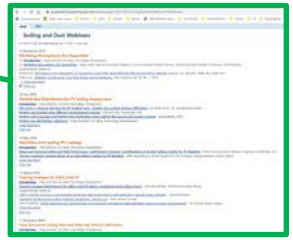

Task Group 12-1 (sensors and the monitoring of soiling)
- ✧ Contributed to IEC 61724-1 (quantifying effect of soiling on PV systems).
- ✧ Interest in interlaboratory precision study.
- ✧ Contact: Bing GUO <bing.guo@qatar.tamu.edu>.

Task Group 12-2 (solutions for **cleaning**)
- ✧ Module cleaning best practices (manual & robotic methods).
- ✧ Reference: Einhorn et. al., IEEE J PV, 9 (1), 2018, 233-239.
- ✧ Contact: Lin SIMPSON <Lin.Simpson@nrel.gov>

Task Group 12-3 (antireflective and/or anti-soiling **coatings**)
- ✧ Focus on PV abrasion methods, developing: IEC 62788-7-3.
- ✧ References: Miller et. al., J PV, 10 (1), 2020, 173-180. (paper, presentation) http://www.nrel.gov/docs/fy16osti/66334.pdf
- ✧ Contact: David MILLER <David.Miller@nrel.gov>

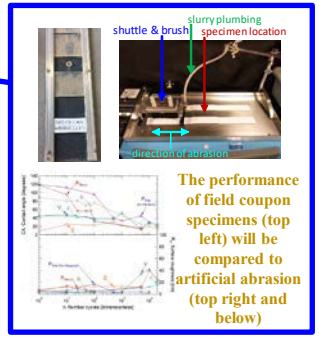

Task Group 12-4 (**modeling/analysis** of effects of soiling on **PV systems**)
- ✧ Example soiling-loss & -rate from PV installation power production data.
- ✧ Reference: Deceglie et. al., Proc. IEEE J PV, 2018.
- ✧ Contact: Leo MICHELI <lmicheli@ujaen.es>

See: http://www.pvqat.org (PVQAT effort) **also: http://pvqataskforceqarating.pbworks.com (minutes, references, attachments, meeting recordings. Contact: David.Miller@nrel.gov)**

IEC 62788-7-3 (PV Abrasion) Standard Is Under Development

•Upon review, no existing standard from other industries was found readily suited for PV.
-Example: frosted –glass- specimens. See: Miller et. al., NREL/TP-5J00-66334, 2016, 1-25.
⇒Accelerated abrasion standard for PV surfaces is presently being developed in IEC WG2.

Methods

•Artificial machine abrasion.
-**Cleaning** of PV (front surface coatings & VIPV).
-Includes slurry or dry dust abrasive.
-Linear translation or rotating brush.

•Falling sand test.
-Natural abrasion (wear from typical meteorological conditions).
-Front surface coatings & backsheets.

•Forced sand impingement test.
-Covers severe storms (infrequent, but high velocity wind).
-Front surface coatings & backsheets & vehicle integrated PV.

☞If you would like to join/follow the project team,
Contact: David.Miller@nrel.gov

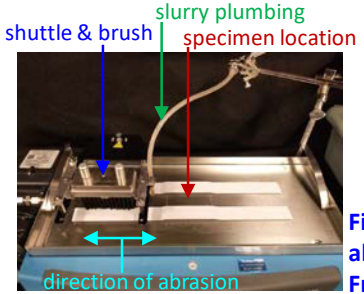

Fixture for (slurry) linear machine abrasion test.
From Miller et. al., J PV, 2019.

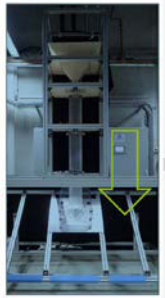

Fixture for falling sand test. From Mathiak et. al., Proc. EU PVSEC 2018.

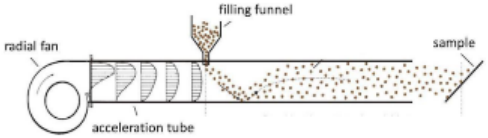

Schematic of forced sand impingement test. From Klimm et. al., Proc. Euro. Weathering Symp. 2015.

Acknowledgements

👍Thanks to: Telia Curtis, Pr. Govindasamy Tamizhmani of ASU; Jean-Nicolas Jaubert, George Kuo, and Ruirui Lv of Canadian Solar; Aaesha Alnuaimi, Pedro Banda, Jim J. John, Marco Stefancich of DEWA; Ben Bourne, Zoe Defreitas, Fabrizio Farina, Greg Kimball, of Sunpower; Anil Kottantharayil, Juzer Vasi, Sonali Warade of IIT-Bombay; Bader Alabdulrazzaq and Ayman Al-Qattan of KISR.

☺ If interested in the PVQAT TG12-3 activities or IEC 62788-7-3 PV abrasion standard, please contact: David.Miller@nrel.gov Participants wanted. ☺

Funding was provided as part of the Durable Modules Consortium (DuraMAT), an Energy Materials Network Consortium funded under Agreement 32509 by the U.S. Department of Energy (DOE), Office of Energy Efficiency & Renewable Energy, Solar Energy Technologies Office (EERE, SETO). This work was authored in part by the NREL, operated by Alliance for Sustainable Energy, LLC for the US DOE under contract no. DE-AC36-08GO28308. Part of this work was performed at the Stanford Nano Shared Facilities (SNSF), supported by the National Science Foundation under award ECCS-1542152.
The views expressed in the presentation do not necessarily represent the views of the DOE or the U.S. government. Instruments and materials are identified in this paper to describe the experiments. In no case does such identification imply recommendation or endorsement by NREL.

NREL STM campus (Dennis Schroeder)

Appendix

Additional slides follow for reference

Goals of This Study

- Determine coating failure modes.
- Identify characterization methods that can detect nascent failures.
- Compare the durability of popular contemporary coating materials subject to linear artificial brush abrasion.
- Compare the damage characteristics for artificial machine abrasion to those observed in a separate field coupon study.
- Compare the rate- and subsequent damage characteristics between wet and dry dust abrasion.
- Compare the rate- and subsequent damage characteristics for factors affecting abrasion (.i.e, use of no abrasive or use of a compliant brush).
- Support the development of an abrasion test standard for the PV industry.

Representative Performance of J Glass (No Coating) in Slurry Abrasion

- Variation shown for $n \leq 20000$ for 1 S.D.
- Representative data (and variation) for stable material shown through greatest cumulative cycle count examined.
- $\tau_{d,rsw}$ & *YI*, do not change within variability of measurement.
- *CA* decreased (increased hydrophilicity, including from cleaning of glass surface).
- R_a increased at greatest cycle count, approaching triple that of baseline value.

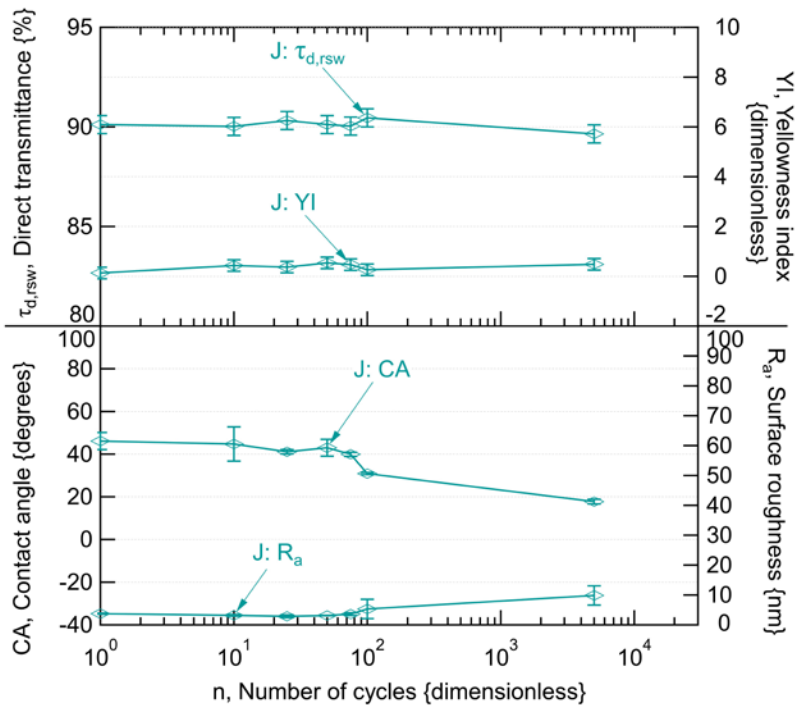

Comparison of transmittance, yellowness index, surface energy, and surface roughness (average) with the cumulative brush cycle count (up to n = 20000) for specimen J (*glass with no coating*).

Coating Degradation Results From Localized Damage Accumulation

- No shift in spectral region of greatest τ_d & no $\Delta\lambda_{cUV}$ observed for specimen Z.

-Consistent with localized damage of a stacked dielectric film coating rather than uniform thickness reduction.

- Specimens with coating not thick enough to realize a gradual wear (with a net change in thickness), unlike specimen A (monolithic PMMA).

-Accumulation of localized damage dominates the degradation of the specimens with a coating (specimens B, E, P, V, and Z).

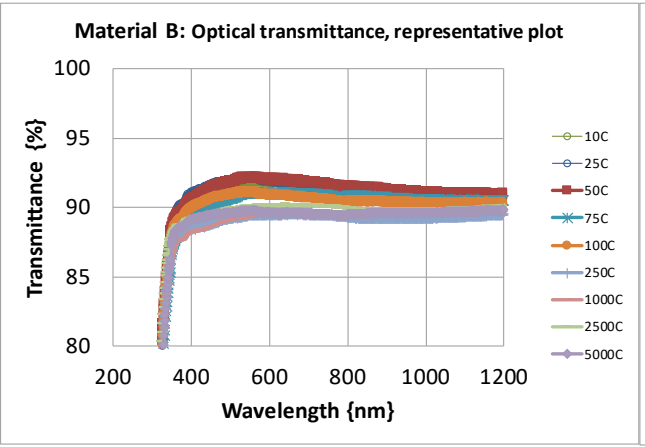

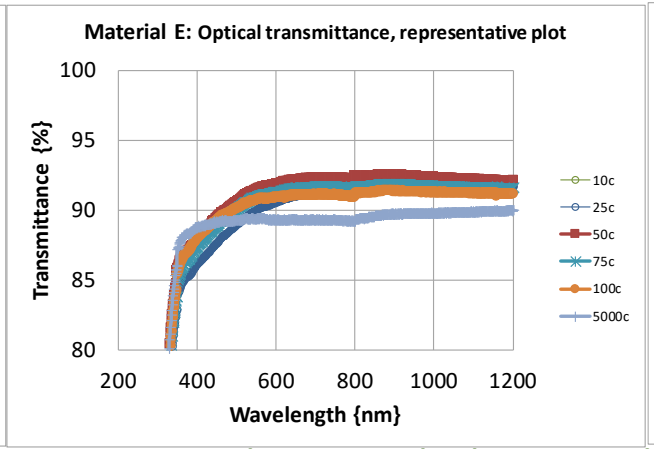

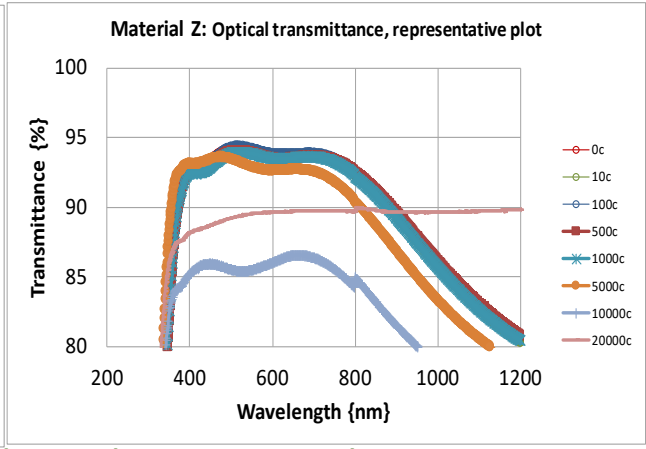

Direct transmittance through the abrasion experiments for B (porous silica), E (porous silica), and Z (stacked dielectric) coatings.

Appendix: Surface Morphology (Scratch Width and Depth) For Select Specimens

- Representative AFM images are shown at same scale (200 nm).

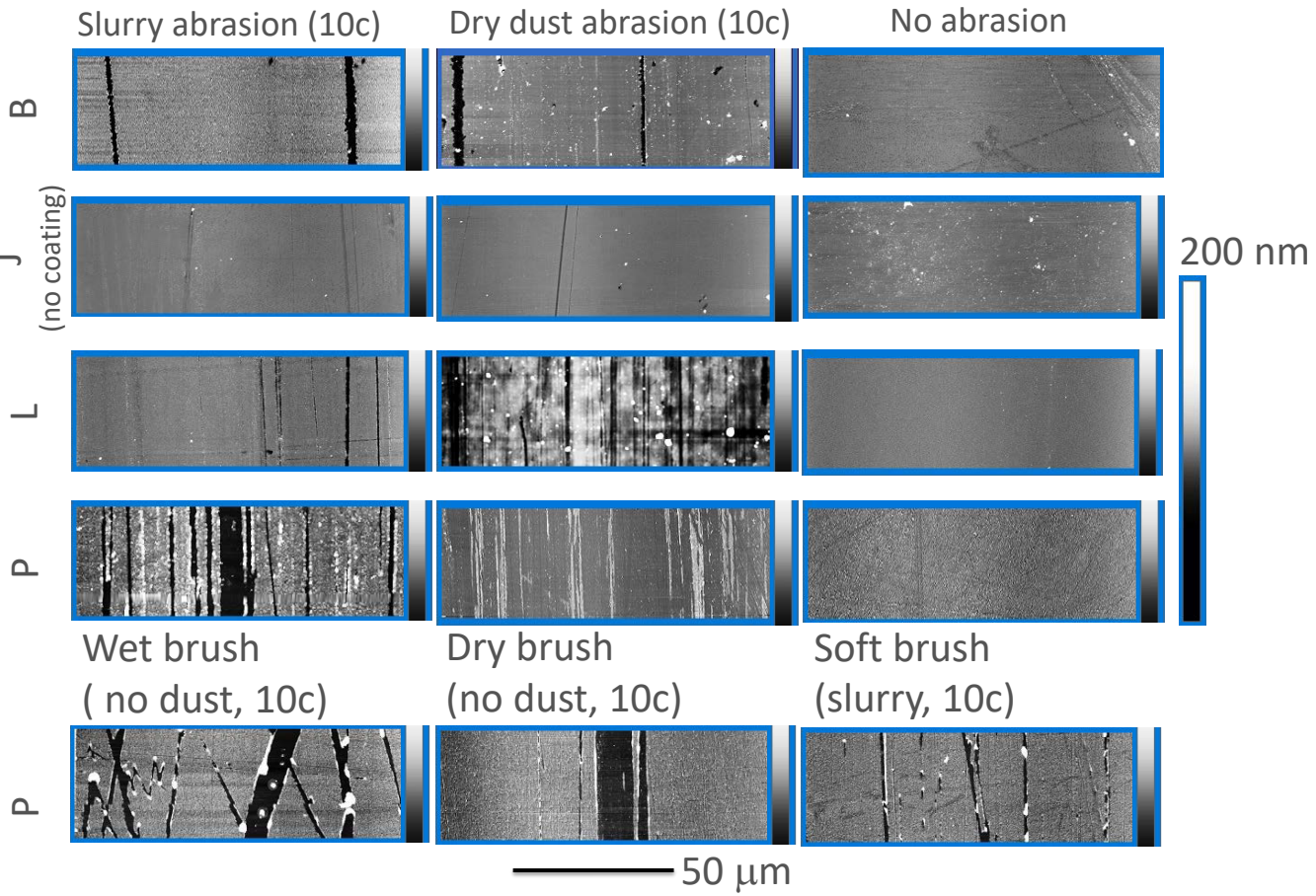

Appendix: Surface Morphology (Scratch Width and Depth) For Select Specimens

- Representative AFM images are shown at same scale (200 nm).

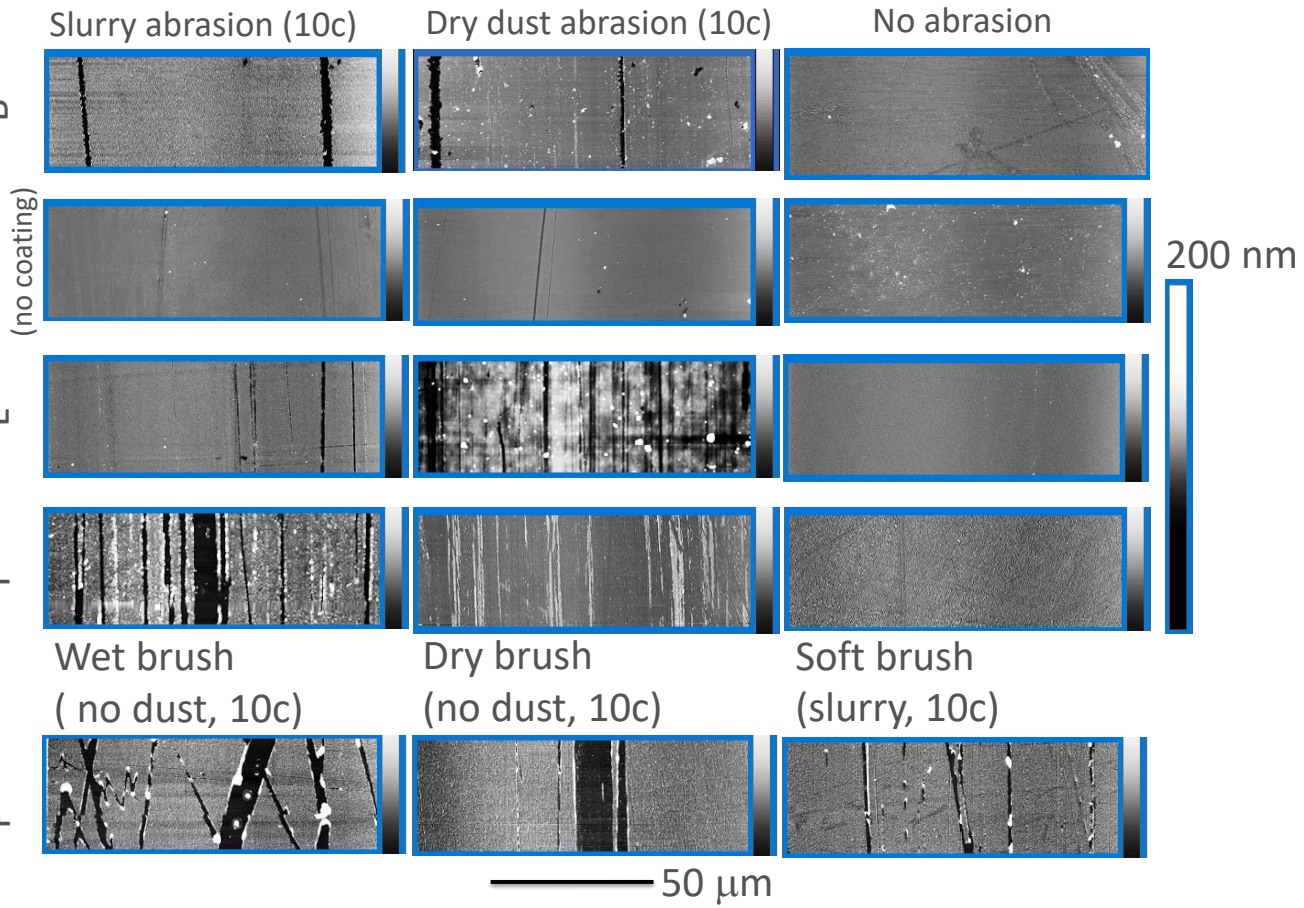

Appendix: Optical Microscopy (Representative Images For Dry Dust, From 100x)

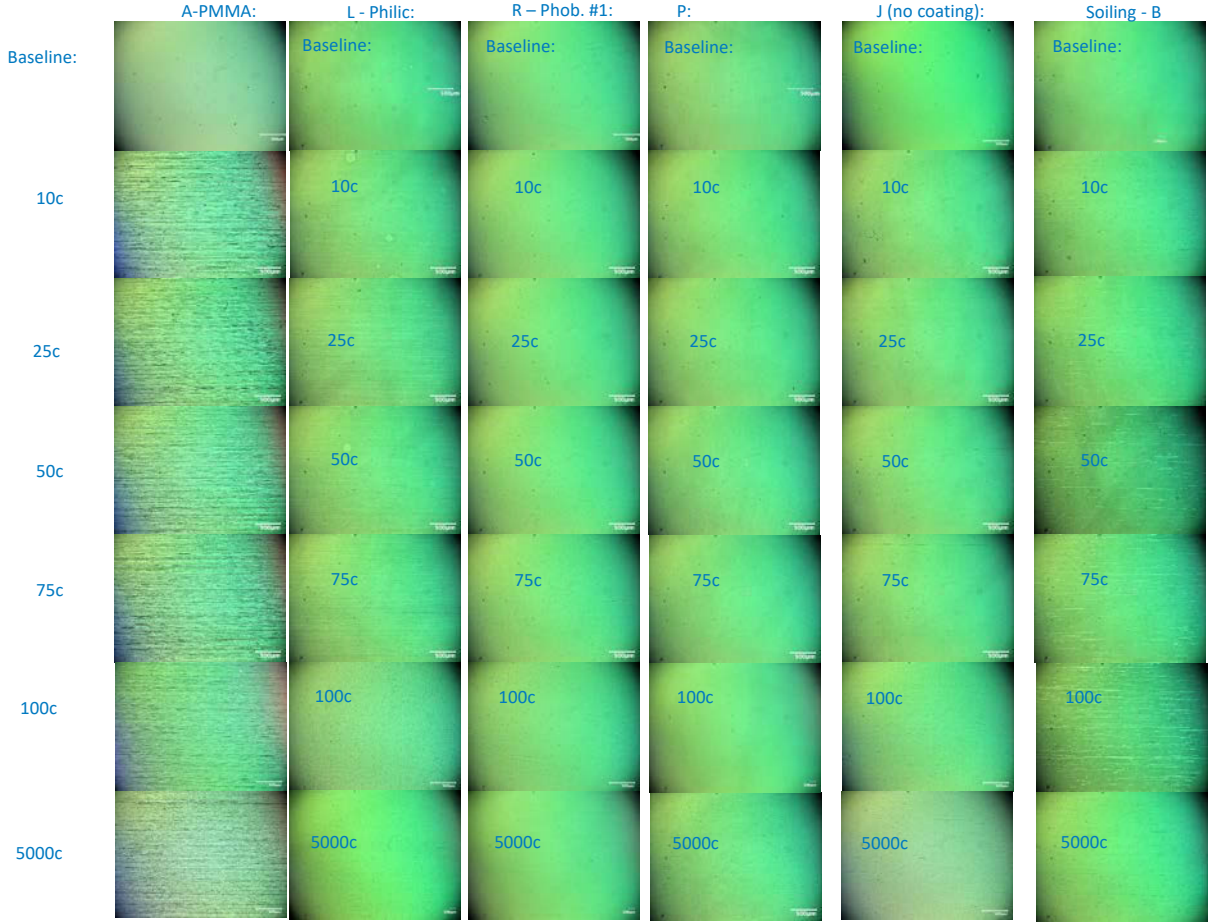

Appendix: Optical Microscopy (Representative Images For Dry Dust, From 500x)

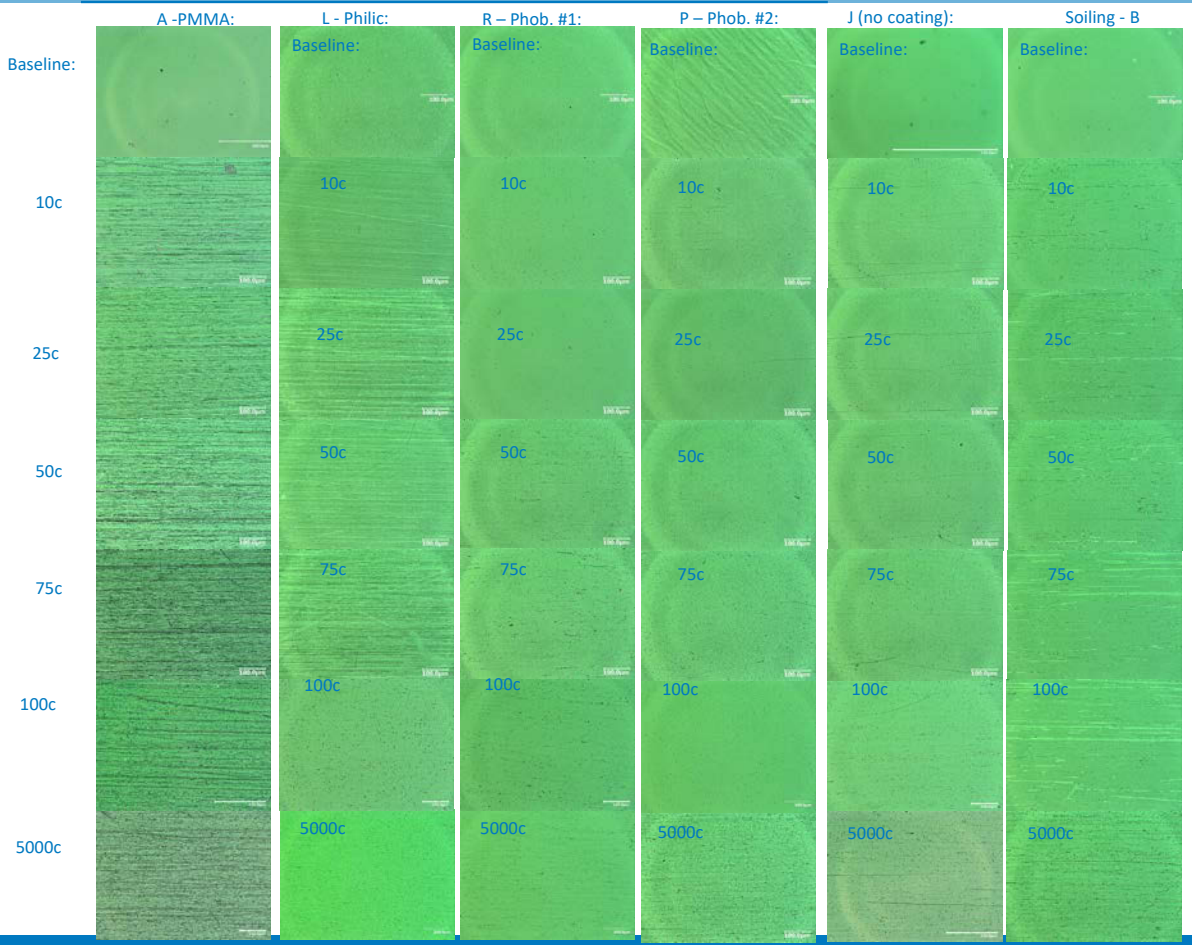

Appendix: Optical Microscopy (Representative Images For Slurry, From 500x)

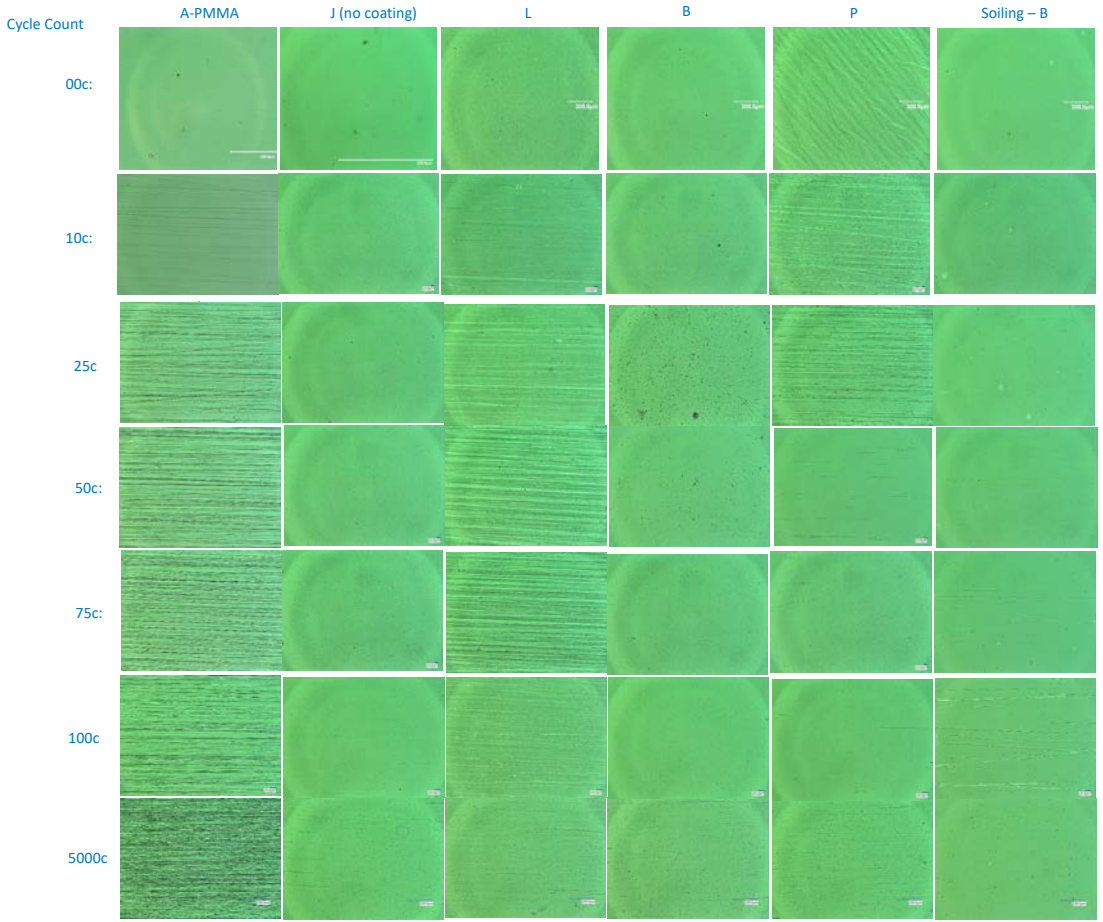

Appendix: Optical Microscopy (Representative Images For Slurry, From 500x)

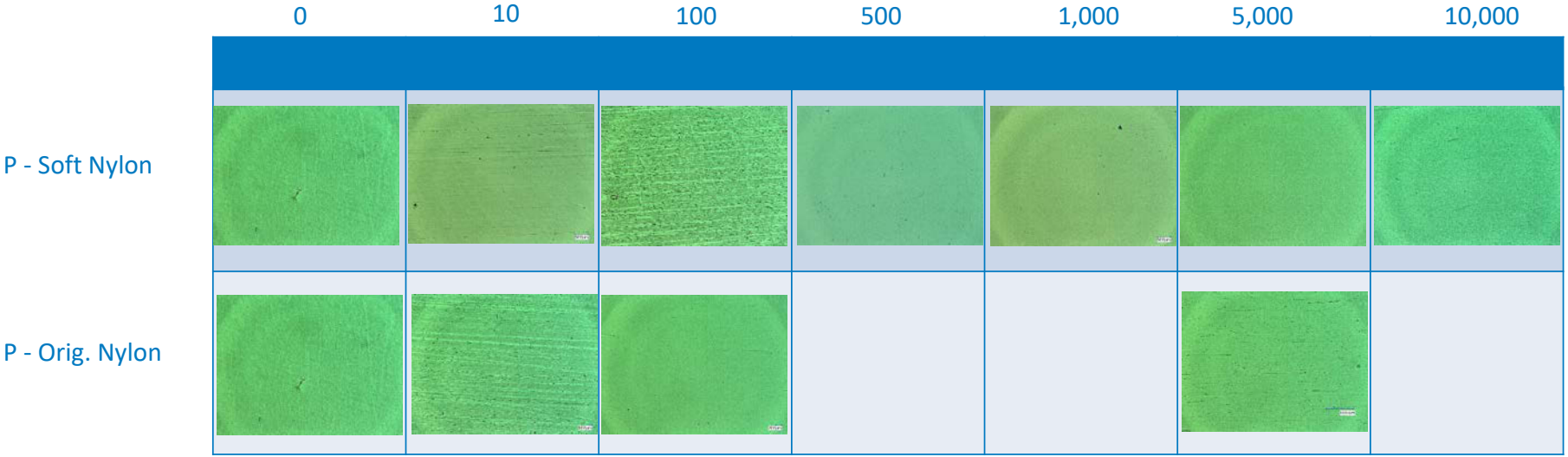

Appendix: Optical Microscopy (Representative Images For Slurry, From 500x)

	00	10	100	500	1000	5000	10000
P – Dry – No Dust	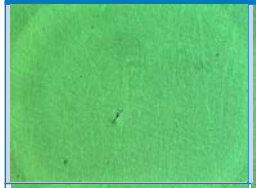					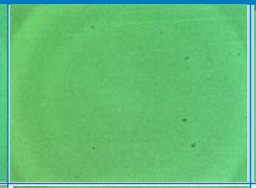	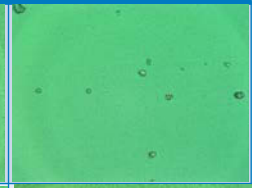
P – Water – No Dust	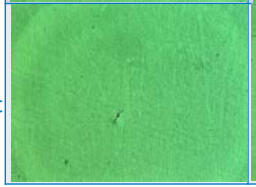	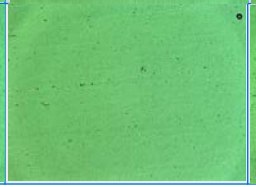	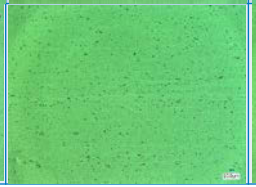			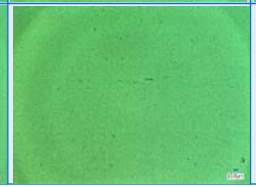	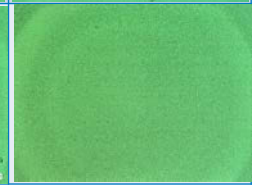

Appendix: Optical Microscopy (Representative Images For Slurry, From 500x)

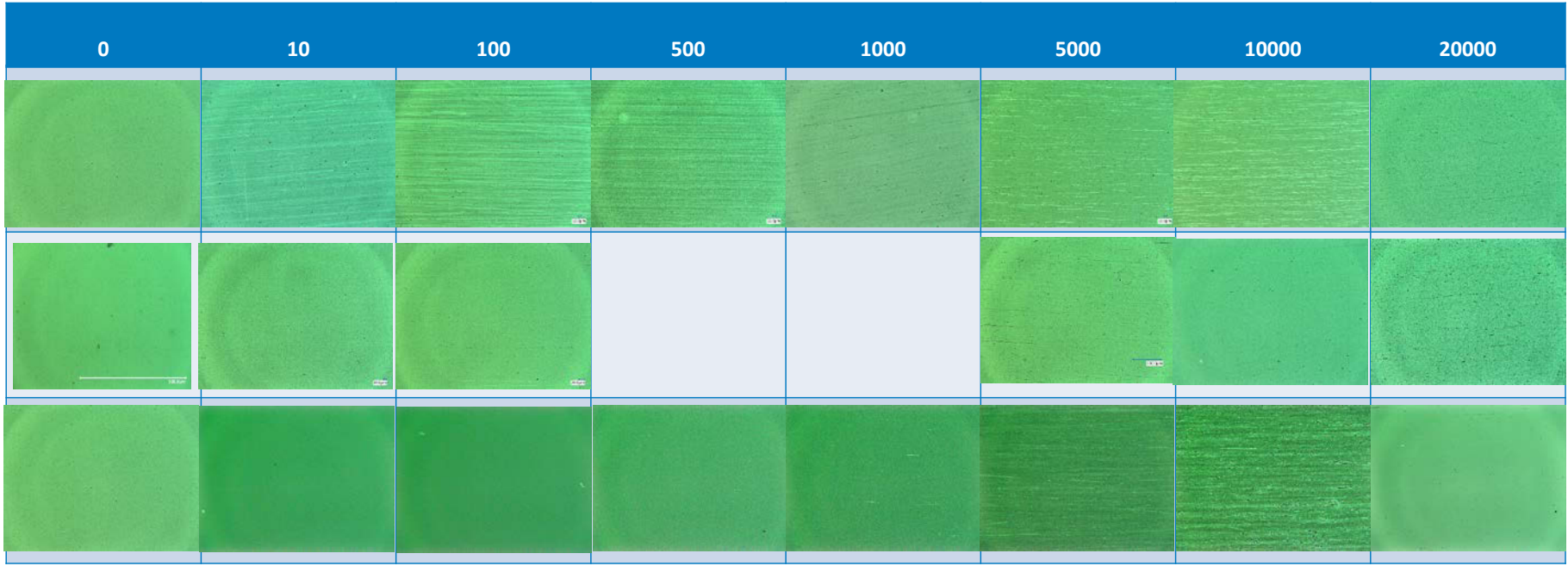

Supplemental Material: Slurry Abrasion

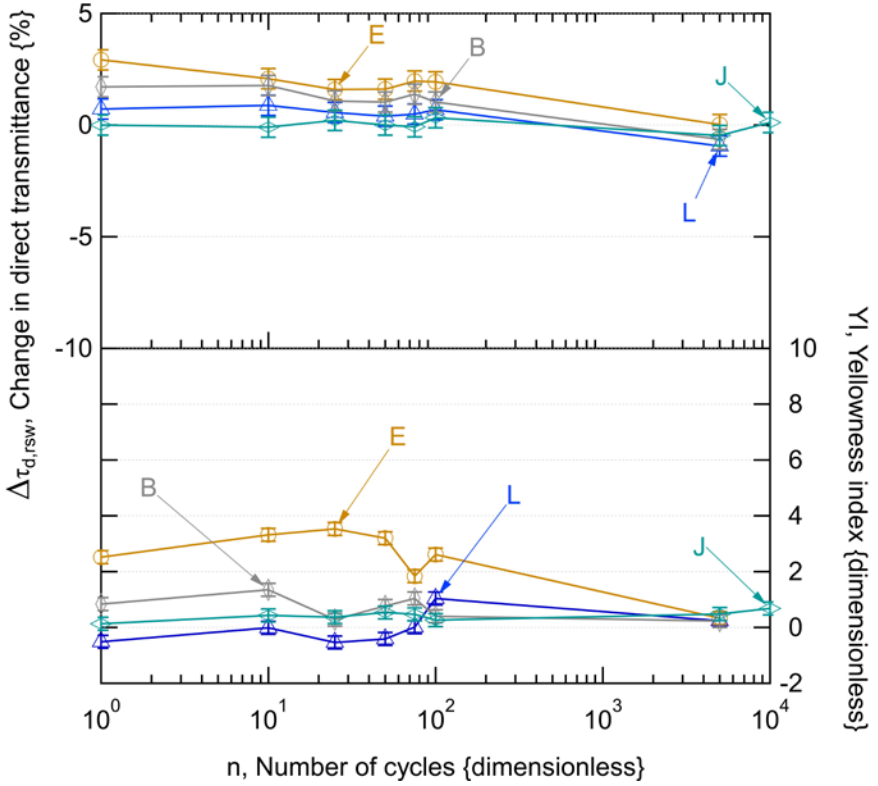

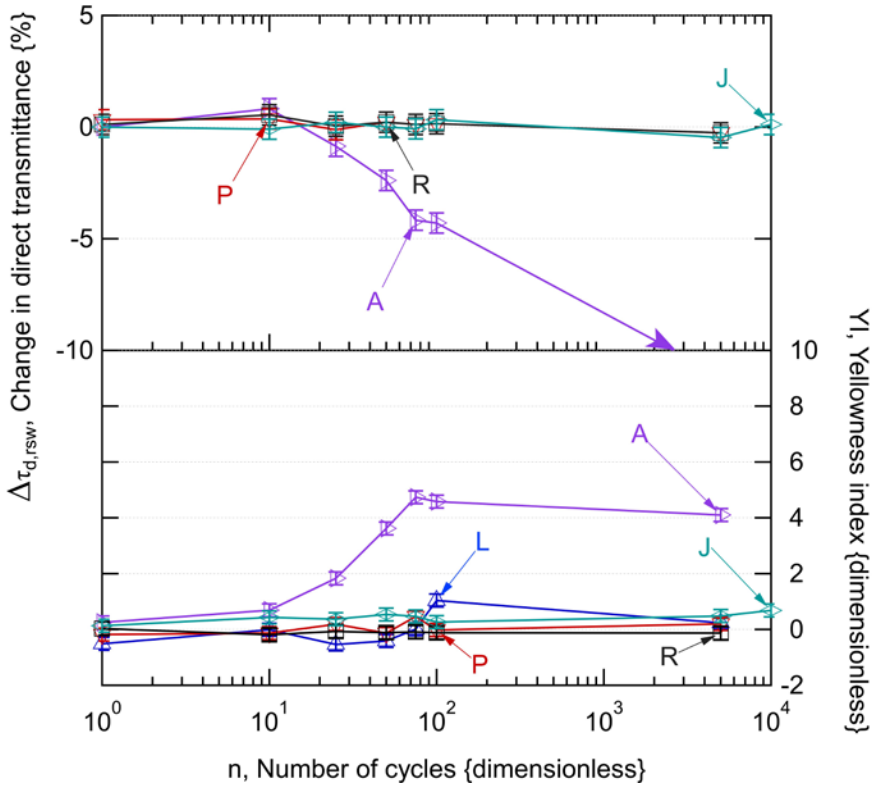

Comparison of the change in transmittance (i.e., coating optical performance) and yellowness index (which may vary with optical scattering) with the cumulative brush-cycle count ($n \leq 5000$) for select coatings for artificial linear brush abrasion with slurry. The precision of the spectrophotometer is shown (2 S.D.), relative to the single measurement of each specimen (sample area of ~1 cm^2).

Supplemental Material: Slurry Abrasion

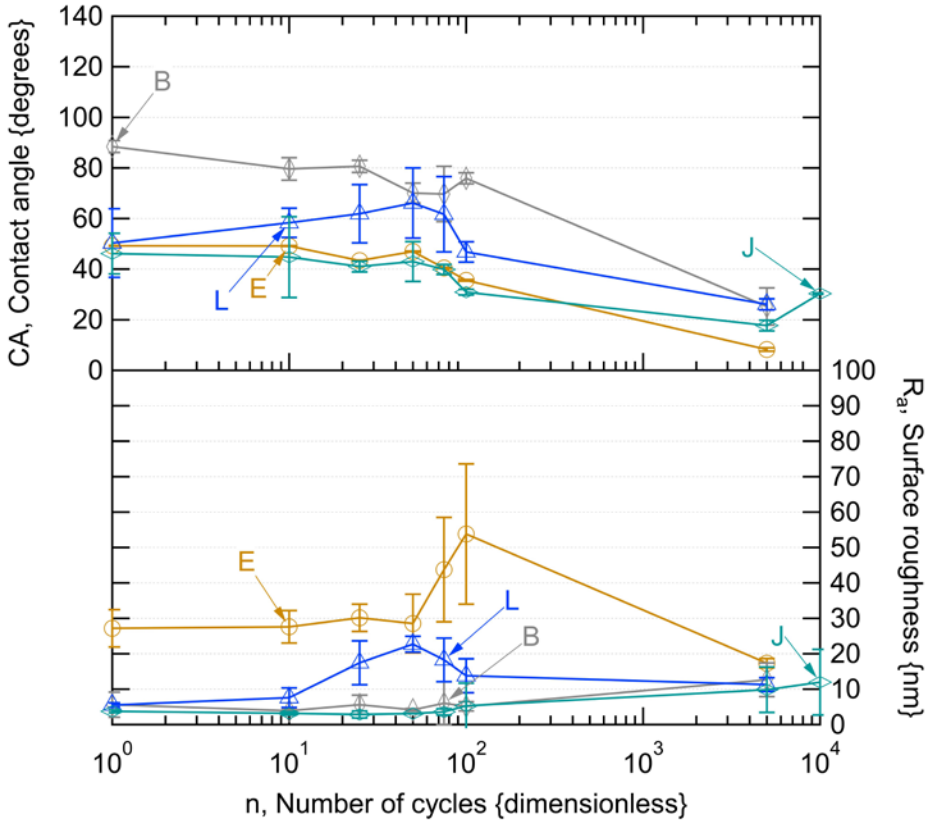

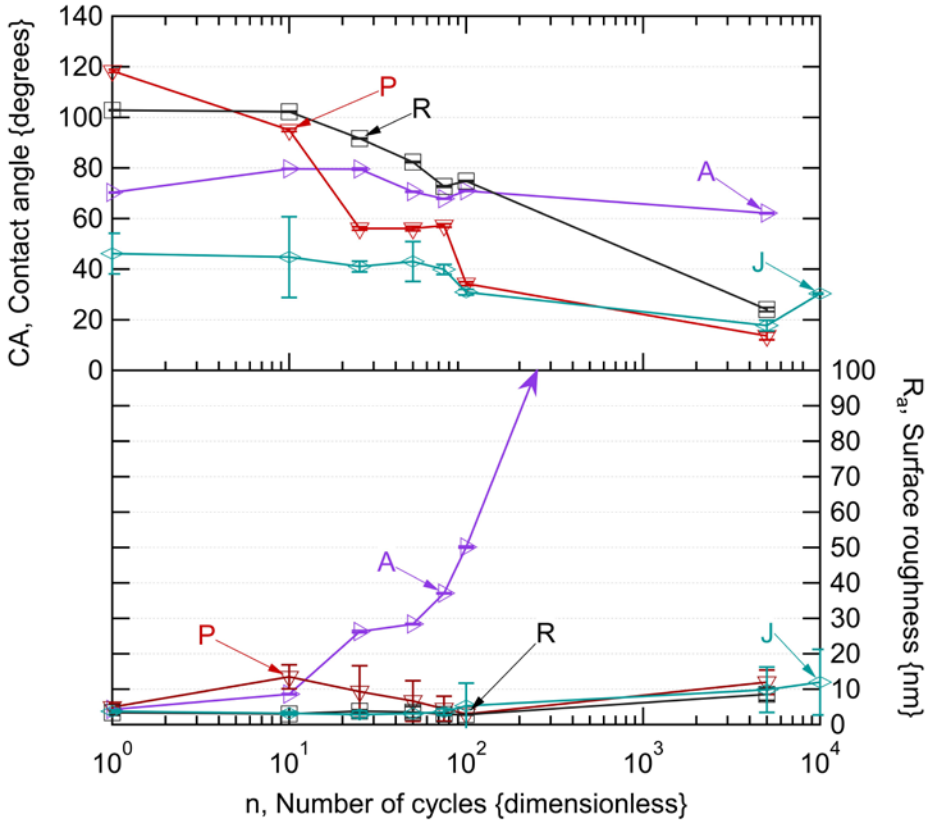

Comparison of the change in surface energy (contact angle for water) and average surface roughness with the cumulative brush-cycle count (n ≤ 5000) for select coatings for linear abrasion with slurry. The variation of the measurements is shown (2 S.D.), at the read point for each specimen (thirty measurements for CA and five area scans for R_a).

Supplemental Material: Dry Dust

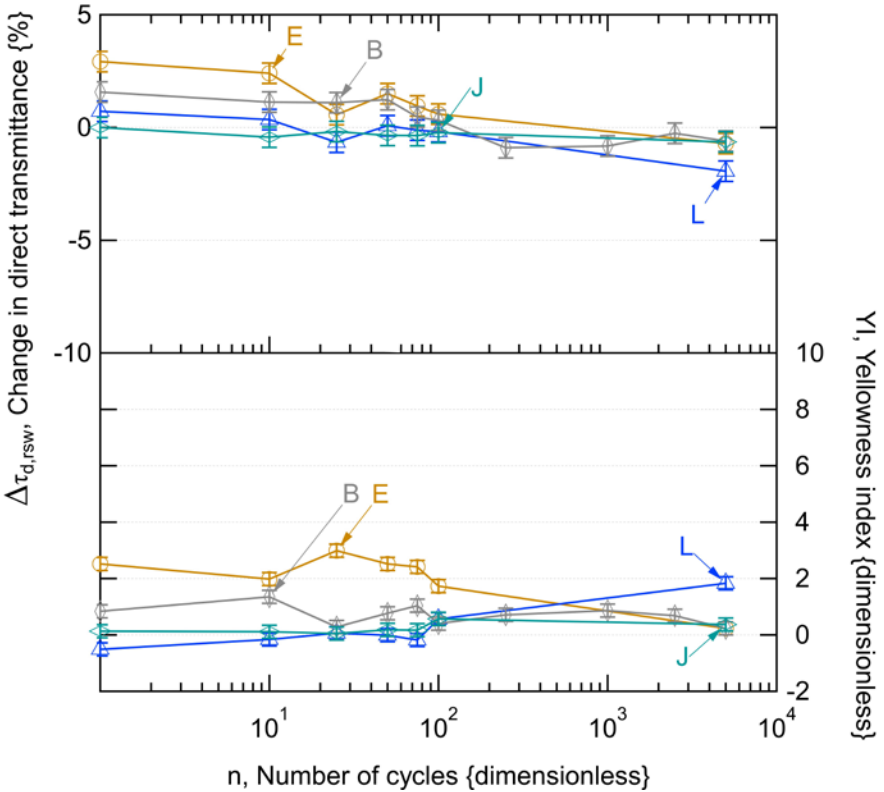

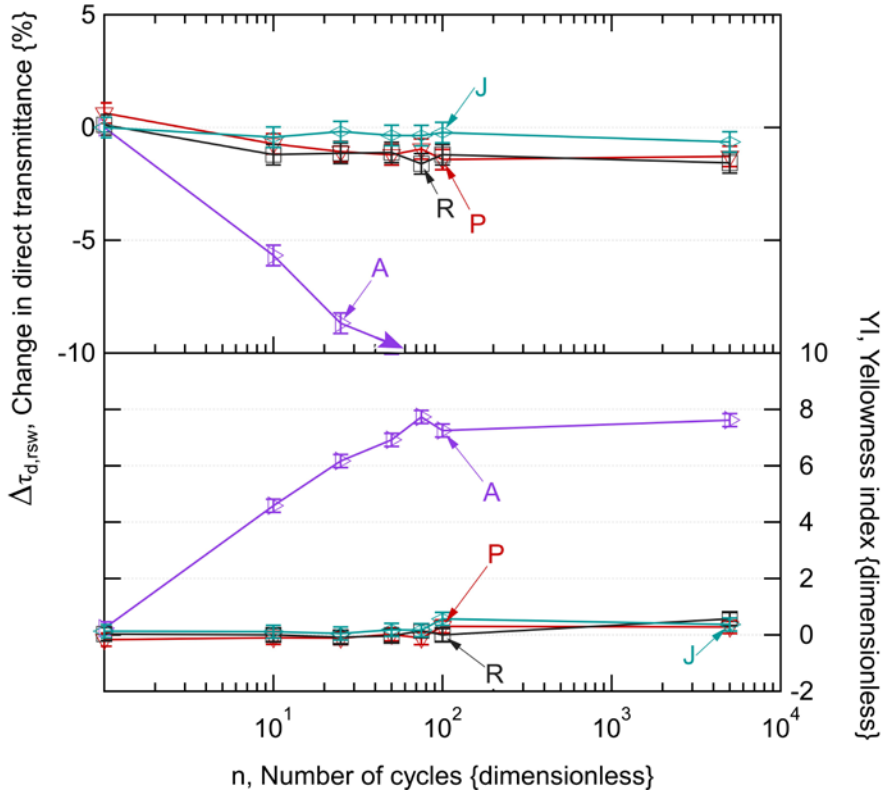

Comparison of the change in transmittance and yellowness index with the brush-cycle count ($n \leq 5000$) for select coatings for linear abrasion with dry-dust. The precision of the spectrophotometer is shown (2 S.D.), relative to the single measurement of each specimen (sample area of ~1 cm^2).

Supplemental Material: Dry Dust

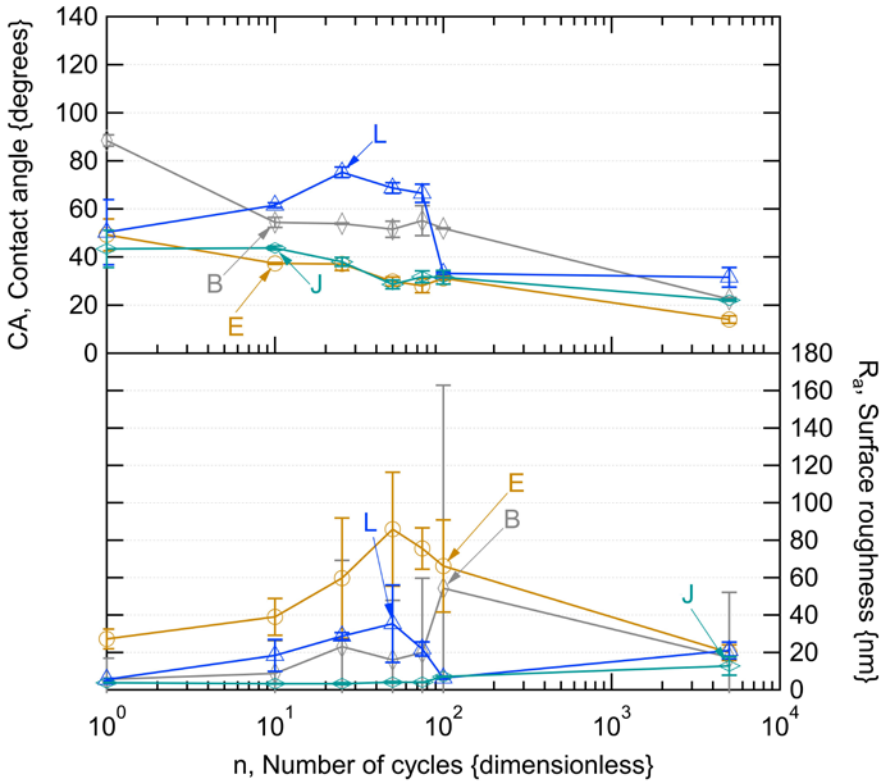

Comparison of the change in surface energy (contact angle for water) and average surface roughness with the cumulative brush-cycle count (n ≤ 5000) for select coatings for linear abrasion with dry dust. The variation of the measurements is shown (2 S.D.), at the read point for each specimen (thirty measurements for CA and five area scans for R_a). Unlike other similar figures in this study, the scale for has been set for Ra to show the data and its variation.

Supplemental Material: P Specimens

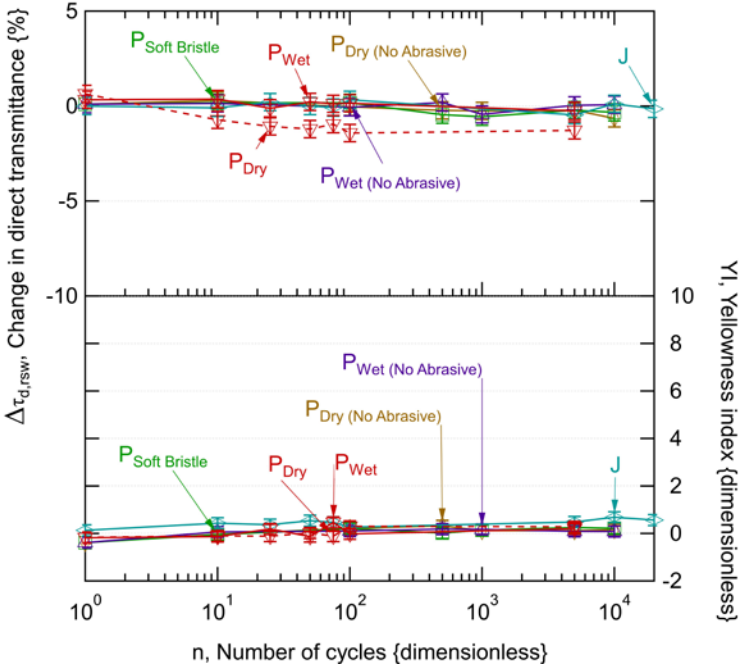

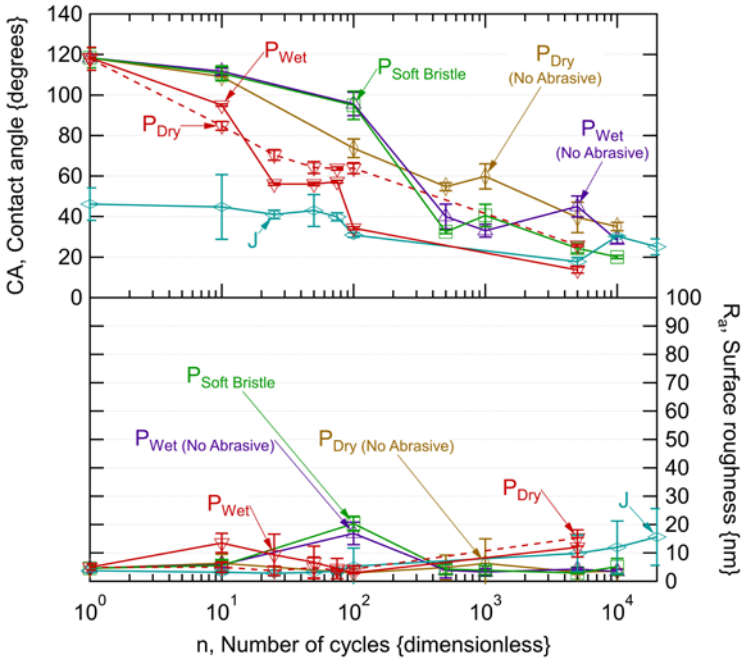

Left: Comparison of the change in transmittance and yellowness index with the brush-cycle count (n ≤ 20000) for select abrasion experiments. The precision of the spectrophotometer is shown (2 S.D.), relative to the single measurement of each specimen (sample area of ~1 cm^2).

Right: Comparison of the change in surface energy and surface roughness with the brush-cycle count (n ≤ 20000) for select experiments. The variation of the measurements is shown (2 S.D.), at the read point for each specimen (thirty measurements for CA and five area scans for R_a).

Supplemental Material: Select Specimens

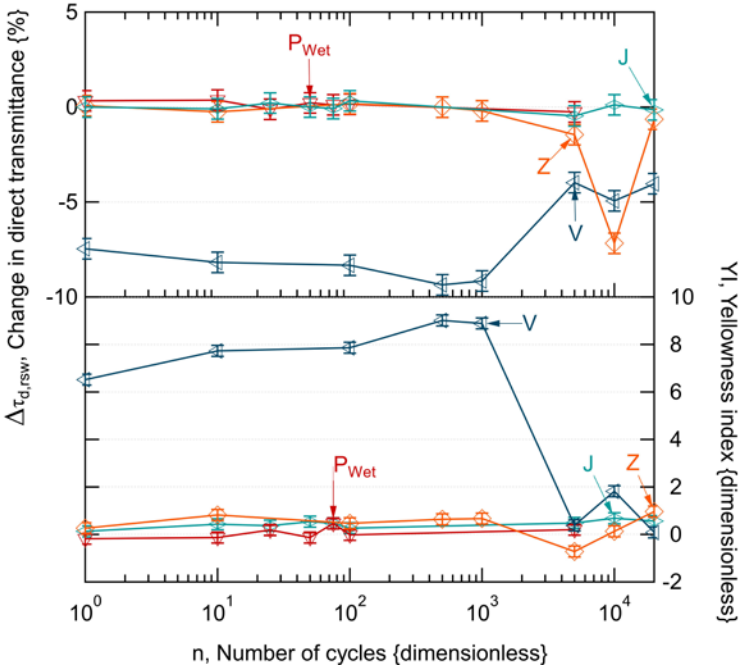

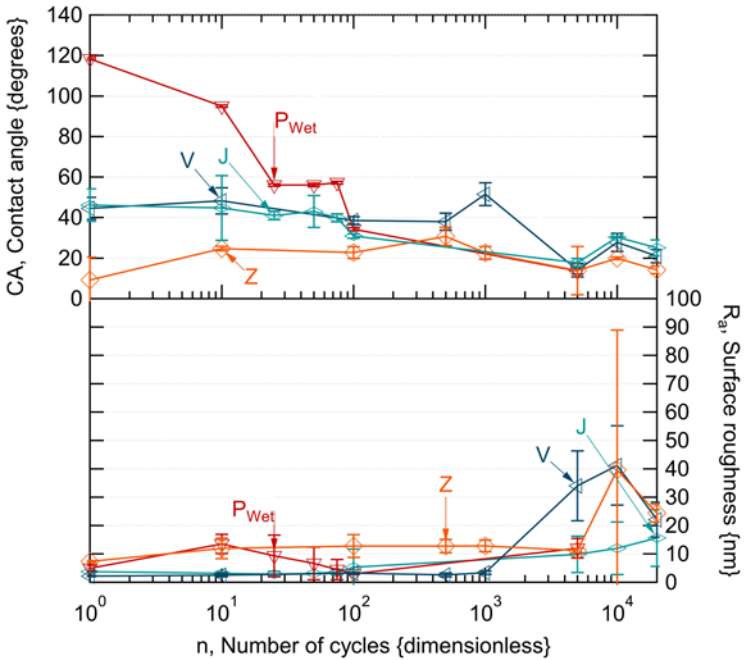

Left: Comparison of the change in transmittance and yellowness index with the brush-cycle count (n ≤ 20000) for select experiments for abrasion with slurry. The precision of the spectrophotometer is shown (2 S.D.), relative to the single measurement of each specimen (sample area of ~1 cm^2).

Right: Comparison of the change in surface energy and surface roughness with the brush-cycle count (n ≤ 20000) for select experiments for abrasion with slurry. The variation of the measurements is shown (2 S.D.), at the read point for each specimen (thirty measurements for CA and five area scans for R_a).

Summary of Glass Composition From XPS Depth Profiling Measurements

"surface" measurements

			CONCENTRATION {% atomic}								
GLASS	SURFACE	DEPTH {nm}	Al	C	Ca	Fe	Mg	Na	O	Si	Sn
Solite	sun (rolled smooth)	3	0.7	0.2	1.4	0.0	0.3	0.6	56.7	39.5	0.0
Solite	cell (stipple)	3	1.0	0.2	1.9	0.0	0.5	0.6	39.5	56.2	0.0
Diamant	sun (Sn-rich)	3	0.3	0.0	1.0	0.7	0.4	1.1	56.2	39.1	1.1
Diamant	cell (Sn-poor)	3	0.5	0.4	0.4	0.0	0.4	0.3	56.0	42.0	0.1

sub-surface ("bulk") measurements

			CONCENTRATION {% atomic}								
GLASS	SURFACE	DEPTH {nm}	Al	C	Ca	Fe	Mg	Na	O	Si	Sn
Solite	sun (rolled smooth)	AVG[50-70] ±2 S.D.	0.7±0.2	0.0±0.0	2.4±0.1	0.0±0.0	0.8±0.1	2.2±0.2	56.3±0.6	37.6±0.8	0.0±0.0
Solite	cell (stipple)	AVG[50-70] ±2 S.D.	1.4±0.2	0.0±0.0	3.1±0.1	0.0±0.1	1.2±0.1	2.9±0.2	37.6±0.4	53.7±0.4	0.0±0.0
Diamant	sun (Sn-rich)	AVG[50-70] ±2 S.D.	0.3±0.2	0.0±0.0	2.4±0.1	0.2±0.1	1.0±0.1	2.0±0.1	55.9±0.8	37.9±0.8	0.3±0.0
Diamant	cell (Sn-poor)	AVG[50-70] ±2 S.D.	0.4±0.1	0.0±0.0	2.0±0.1	0.0±0.1	1.0±0.1	2.0±0.1	55.3±01.1	39.2±1.0	0.0±0.0

Discussion

- The change in τ_d, *YI*, *CA*, and R_a as well as morphology in optical microscopy is consistent with the processes of damage initiation, damage accumulation, followed by destruction of the film, with eventual convergence of characteristics observed for the glass substrate.
- Damage to the coatings might be analyzed using machine cutting tool model (to represent localized erosion) rather than analysis based on the tribological wear of a bulk material.
- Linear artificial brush abrasion method improved relative to previous study: A4→A3 test dust (more similar to field contamination); longer bristles (as in commercial brushes for PV).
- Limitations: other materials and cleaning equipment presently used to clean PV systems, including: synthetic & natural fibers, sponge, and micro-fiber fabric. Rotating cleaning equipment is presently popular in automated/robotic cleaning systems.
- Equipment-, method-, and site specific-validation as well as the corresponding site-specific acceleration factor for the test method, however, remain to be established. Industry-level effort required.